e-ISSN: 2349-9745
p-ISSN: 2393-8161
Scientific Journal Impact Factor (SJIF): 1.711
International Journal of Modern Trends in Engineering and Research
www.ijmter.com

# WHEEL SLIP CONTROL OF ELECTRIC VEHICLE WITH CONDITIONAL CONTROLLER

Arun pandian. S[1], Mr. Murali Babu. B, M.E.[2]
[1,2]Paavai Engineering College/EEE Dept, Namakkal, India

**Abstract**—The precise position control, of multi-motor electric vehicles (EVs) by generating the asymmetric pulse generation is presented. The energy saving algorithm is implemented in the power drain control of EV system to improve the electrical safety and slip control of electric vehicle. The acceleration and Deceleration of the electric vehicle for wheel slip control were analyzed using the parameters like voltage, speed, torque. The result obtained of the proposed wheel slip controller with phase control modulation is presented and the Experimental results, obtained with a multi-motor EV prototype under low grip conditions, demonstrate a good slip regulation.

**Index Terms—**Electric vehicles (EVs), field programmable gate array (FPGA), Powerdrain control, sliding mode control (SMC),Induction Motor, voltage source inverter(VSI),traction control (TC).

## I. INTRODUCTION

Early from1990s there has been resurgence in electric vehicles (EVs) research, stimulated by various factors such as rising oil prices, environmental concerns, cost reduction of power electronics and motor drives, and a marked improvement in energy storage technologies. EV is based on three fundamental concepts: 1) controller reconfigurability; 2) energy efficiency; and 3) safety. To tacklethis challenge recent development of power electronics has led to an increased interest in voltage source inverters with pulse width modulation control of AC drives. The voltage can be produced at desired output frequency and voltage level by using inverters. The adhesion control between the tyre and road has been divided into two classes of driving aid systems. They are traction control (TC), enabled during accelerating maneuvers and the antilock braking system (ABS), active during decelerations. The motivation for introducing these systems is related to the difficulty that the drivers experience in controlling the throttle/brake pedal when the vehicle is running over slippery surfaces, such as moisture. In these conditions, it is tricky for the drivers to judge how much wheel torque to apply, and it is common to end up employing excessive wheel torque that results in skid (braking) or high tyre spin (acceleration), compromising the longitudinal force generation and reducing the ability of the tyre to transmit lateral forces. The traditional hydraulic-based friction brakes used in the conventional ABS are inherently slow and prone to exhibit limit cycles [1].On the other hand, for four-wheel drive or for braking maneuvers, the $\lambda$ measure is difficult to acquire, because all the vehicle wheels are being driven, which obliges the application of observers for estimating the vehicle speed [2], [3], complicating the controller implementation and tuning. For instance, the linear proportional integral (PI) control proposed in [4], [5] is simple and very attractive from an implementation point of view, but suffers from the fact that the PI tuning is based on a linearization of the quarter-car model (QCM), thus only local stability can be ensured, and robustness to model uncertainty is a concern. The former problem can be attenuated by employing SMC in conjunction with observers, based on neural networks [6], fuzzy logic [7], recursive least squares [8], or sliding modes [9], but they also increase the implementation complexity and the controller tuning effort, and it may be difficult to ensure a fast learning rate in real scenarios. In practice, FPGA $\mu(.)$ is subject to a high degree of uncertainty and varies with many factors like road conditions, tyre pressures, temperature, etc. To overcome the chattering issue, which arrives from the discontinuous nature of the slip control, the conditional controller approach was employed, enabling a smooth

 

transition. When the tyre slip is close to the set point, the controller produces discontinuous nature of pulse for the power drain control and to have a good slip regulation.

## II. ELECTRIC VEHICLE MODEL

In this section a brief description of the technological platform employed in the EV power drain control is introduced.The main motivations for developing the Atmel control architecture, shown in Fig. 1, have been the cost and performance issues. The main driving forces behind this paradigm shift are the parallel features and high calculation capacity offered by the controller, which allow pure modularity, i.e., the control modules share the same physical unit, but run in a truly concurrent model.

### A. Propulsion Control Unit (PCU)

The proposed control architecture (Fig. 1) is designed around a reusable intellectual property core, named propulsion control unit (PCU). For each driving wheel of the EV, an individual PCU module is associated, providing the following functionalities: 1) torque and flux control of the electric motor; 2) energy loss minimization; 3) peak friction estimation and 4) wheel SC. The first functionality, the motor controller, using the classiccontrol module is the most computational-intensive block (contains pulse-width modulators, mathematicaltransformation, proportional and integral controllers and demand considerable computational resource ,e.g., the multipliers. Second, the EVenergy efficiency was addressed by implementing an IM loss- minimization algorithm. This algorithm uses the solution of a parameterized IM loss model to select the most efficient flux set point for each motor operating point (speed andtorque).Experiments carried out in our prototypes showed that, under low torque regime, energy savings of up to 10% are achieved.

A 3-phase squirrel-cage motor rated 3 HP, 415V, 50 HZ, 1725 rpm is fed by a 3-phase MOSFET inverter connected to a DC voltage source of 325V. The inverter is modeled using the "Universal Bridge" block and the motor by the "Asynchronous Machine" block. The load torque applied to the machine's shaft is constant and set to its nominal value of constant value or a step function. Speed control of the motor is performed by the "variable voltage" block. The magnitude and frequency of the stator voltages are set based on the position set point. By varying the stator voltages magnitude in proportion with frequency, the stator flux is kept constant**.**

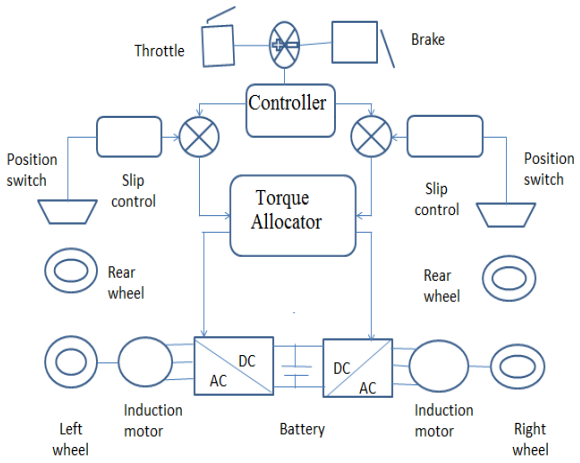


Fig.1 Block diagram of the power drain controller employed in EV prototype

 

## III. ENERGY SAVING ALGORITHM

The goal of a new concept of position control is to create control system satisfying the condition for energy savings. Its basic concept as digitally controlled a.c. drive with prescribed position dynamics is shown in Fig. 1. The input of the control diagram is demanded position and wheel slip position is the controlled output. Overall position control system, usually of cascade structure, can be based on principles of field oriented control (FOC),which would preserve the initial speed and quality of the position control, using optimal input energy of the machine.

As shown in equation (1), electromagnetic torque _T*e* for rotating drives can be written as:

$$Te = TL + J\,{}^{dw}/_{dt} + friction \quad (1)$$

where _T*L* is active load torque, *J* is moment of inertia of the shaft and frictionrepresented total friction of the machine in bearings and in other rotating parts. Friction is therefore characterized as passive load torque. Equation (1) can be written as:

$$Te = TL + J\,{}^{dw}/_{dt} + AW^3 + BW + C \quad (2)$$

Where *A* is windage losses coefficient which takes into account wind resistance by laminar and turbulent flow.Windage losses are generated at the air gap by friction of the air, and also on the fan integrated to shaft, if there exists one. *C* is Coulomb friction coefficient in (*Nm)*. Coulomb friction is independent of speed value, but it changes its signumwith direction of motion. *B* is the viscous friction coefficient in (*Nm.s)* and this type of losses generated in the bearings can be approximated analytically also as (Gieras 1997) (3) in (*W*).

$$Pf = {}^{3kbmrw}/_{100\pi} \quad (3)$$

where*kb* is a factor with value 1-3, mris the mass of the rotor and _ is the mechanical speed. Equation describing the power balance of the mechanical part of the rotating electrical machine can be obtained from (2) as:

$$Tew = TL + T_L w + JW + AW^3 + Bw^2 + Cw \quad (4)$$

Equation (4) shown that, mechanical losses _Pmechmay be divided into friction and windage losses.

$$\Delta Pmech = Aw^3 + Bw^2 + Cw \quad (5)$$

As shown in equation (5) windage losses depend on the third power and friction losses depend on the quadrate of the angular velocity. For position control with best energy strategy, it is necessary to create an algorithm minimizing the velocity peak for a given position change. Velocity peak reduction minimizes mechanical losses _Pmech when the rotor position is changing. In general reference position without peaks in its derivative is the solution.

## IV. VECTOR CONTROL

Vector control is the most popular controltechnique of AC induction motors. In special reference frames, the expression for the machine is similar to the expression for thetorque of the separately excited DC machine. In the case of induction machines, the control is usually performed in the reference frame (d-q) attached to the rotor flux space vector. That's why the implementation of

 

vector control requires information on the modulus and the space angle (position) of the rotor flux space vector. The stator currents of the induction machine are separated intoflux- and torque-producing components by utilizing transformation to the d-q coordinate system, whose direct axis (*d*) is aligned with the rotorflux space vector. That means that the *q*-axis component of the rotor flux space vector is always zero.The rotor flux space vector calculation and transformation to the d-q coordinate system require the high computational power of a microcontroller; a field orientation control is suitable for this task. The following sections describe the space vector transformations and the rotor flux space vector calculation. In adjustable-speed applications, AC motors are powered by inverters. The inverter converts DC power to ACpower at the required frequency and amplitude.Space Vector Modulation (SVM) can directly transform the stator voltagevectors from an α, β- coordinate system to Pulse Width Modulation (PWM) signals (duty cycle values).The standard technique for output voltage generation uses an inverse Clarke transformation to obtain 3-phasevalues. Using the phase voltage values, the duty cycles needed to control the power stage switches are thencalculated. Although this technique gives good results, space vector modulation is more straightforward (validonly for transformation from the α, β-coordinate system).The basic principle of the standard space vector modulation technique can be explained with the help of the power stage schematic diagram depicted in Fig. 2.

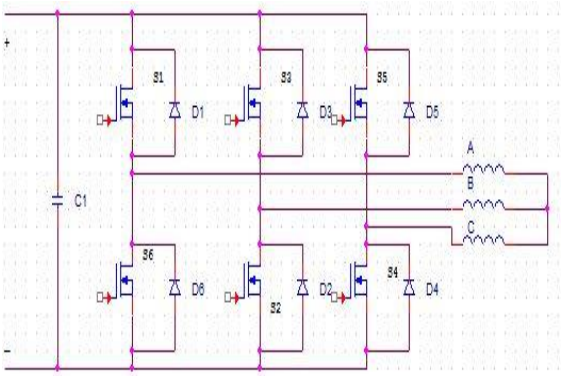


Fig.2 Space Vector Circuit Diagram

In the 3-phase power stage configuration, shown in Fig 3, eight possible switching states (vectors) arepossible and given by combinations of the corresponding power switches. The graphical representation of all combinations is the hexagon shown in Fig 3. There are six non-zero vectors, V1, V2, V3, V4, V5, V6, and two zero vectors, V0and V7.The combination of ON / OFF states of thepowerstage switches for each voltage vector is coded as shown in the Fig.3.

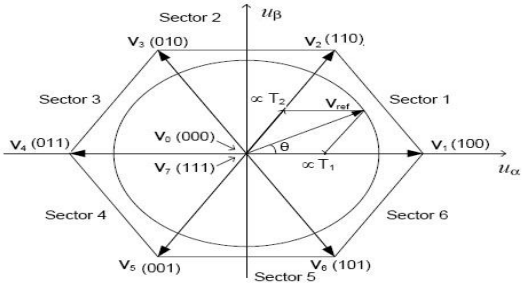


Fig.3 Voltage Vector Projection

For each phase, a value of one means that the upper switch is ON and the bottom switch is OFF. A value of zero means that the upper switch is OFFand the bottom switch is ON. These states, together with the resulting instantaneous output line-to-linevoltages, phase voltages and voltage vectors, are listed in Table 4-1.

 

Table4.1 Switching Patterns

| $V_i$ | A | B | C | $V_{AB}$ | $V_{BC}$ | $V_{BC}$ |
|---|---|---|---|---|---|---|
| $V_0$ | 0 | 0 | 0 | 0 | 0 | 0 |
| $V_1$ | 1 | 0 | 0 | $2V_{DC/3}$ | $-V_{DC/3}$ | $-V_{DC/3}$ |
| $V_2$ | 1 | 1 | 0 | $V_{DC/3}$ | $V_{DC/3}$ | $-2V_{DC/3}$ |
| $V_3$ | 0 | 1 | 0 | $-V_{DC/3}$ | $2V_{DC/3}$ | $-V_{DC/3}$ |
| $V_4$ | 0 | 1 | 1 | $-2V_{DC/3}$ | $V_{DC/3}$ | $V_{DC/3}$ |
| $V_5$ | 0 | 0 | 1 | $-V_{DC/3}$ | $-V_{DC/3}$ | $2V_{DC/3}$ |
| $V_6$ | 1 | 0 | 1 | $V_{DC/3}$ | $-2V_{DC/3}$ | $V_{DC/3}$ |
| $V_7$ | 1 | 1 | 1 | 0 | 0 | 0 |

This method yields the greatest variability of arrangement of the zero and non-zero vectors during the PWM period. One can arrange these vectors to lower switching losses; another might want to approach a different result, such as center-aligned PWM, edge-aligned PWM, minimal switching, etc.

## V. EXPERIMENTAL RESULTS

In this last section, the proposed wheel slip controllers are experimentally validated in the multi-motor EVs prototype, with detailed theory and presentation, as implemented in the digital control system, of discrete pulse with a sampling time of 2 ms, which is quick enough to handle the tire slip dynamics. The vehicle speed, needed for the $\lambda$ calculation, was directly measured using the vehicle non driven wheels. The maximum wheel torque that the driver can request was limited to *Td*= 120N.m, and set equal for both accelerating and braking maneuvers, while the friction brakes weredisabledduring the experiments. In order to assess the controller performance in challenging adhesion conditions, unbalanced condition was artificially created using an experimental apparatus, as shown in Fig.4&5.

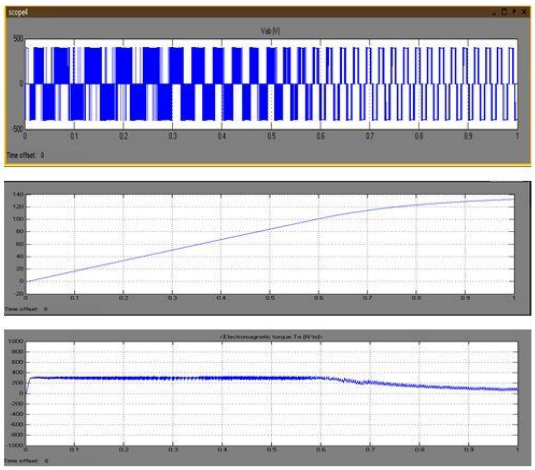

Fig.4 Wave Form For Acceleration

 

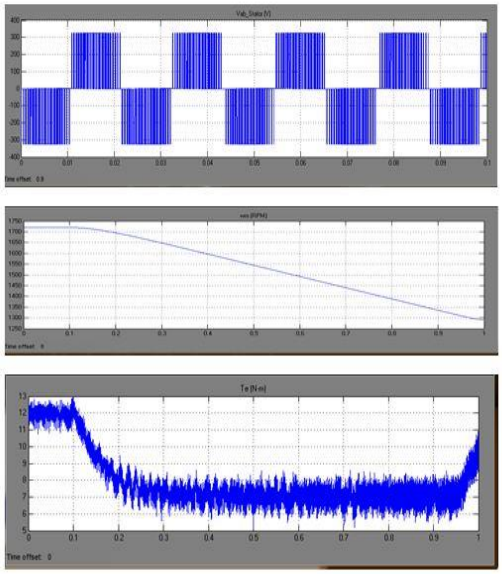

Fig.5 Wave Form For Deceleration

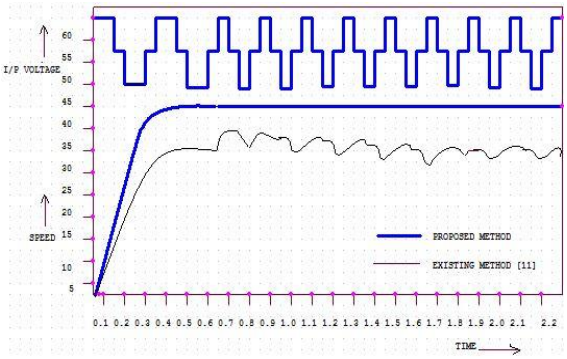


Fig. 6 comparison For Acceleration

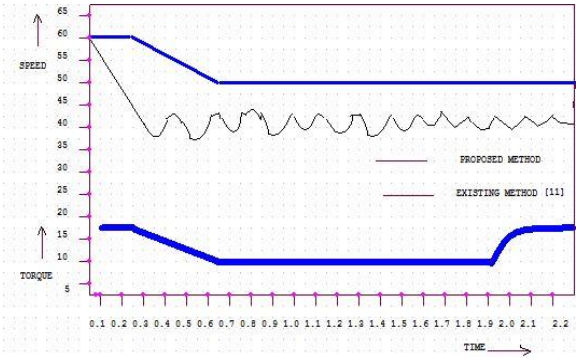


Fig. 7 comparison For Deceleration

When we compare the existing method result with proposed method result. It has greater advantage in saving the input energy with respect to the position control as shown in the Fig. 6. When the slip value is to be critical the speed is decreased to a safer value and the slip is controlled with a safer limit as shown in Fig .7.

## VI. CONCLUSIONS

Presented experimental result confirmed that a wheel slip control with conditional controller can save significant proportion of the drives input energy with respect to the precise position control. The energy saving algorithm implemented in the power drain control of EV system has improved the input energy saving about 10% which increased electrical safety and slip control of electric

 

vehicle.The acceleration and Deceleration of the electric vehicle results were analyzed and presented with balanced parameters like voltage, speed, torque.Experimental results confirmed that proposed controller can bring savings of input energy if compared with step speed response control. It can be easily implemented into control system of existing ac drives.

## REFERENCES

[1] U. Kiencke and L. Nielsen, *Automotive Control Systems For Engine, Driveline, and Vehicle*. New York: Springer-Verlag, 2005.
[2] L. Imsland, T. A. Johansen, T. I. Fossen, H. Grip, J. C. Kalkkuhl, and A. Suissa, "Vehicle velocity estimation using nonlinear observers," *Automatica*, vol. 42, no. 12, pp. 2091–2103, Dec. 2006.
[3] Y. Hori, "Future vehicle driven by electricity and control—Research on four-wheel-motored UOT Electric March II," *IEEE Trans. Ind. Electron.*,vol. 51, no. 5, pp. 954–962, Oct. 2004.
[4] Y. Hori, Y. Toyoda, and Y. Tsuruoka, "Traction control of electric vehicle: Basic experimental results using the test EV 'UOT Electric March'," *IEEETrans. Ind. Appl.*, vol. 34, no. 5, pp. 1131–1138, Sep./Oct. 1998.
[5] L. Chih-Min and C. F. Hsu, "Neural-network hybrid control for antilock braking systems," *IEEE Trans. Neural Netw.*, vol. 14, no. 2, pp. 351–359, Mar. 2003.
[6] L. Chih-Min and C. F. Hsu, "Self-learning fuzzy sliding-mode control for antilock braking systems," *IEEE Trans. Control Syst. Technol.*, vol. 11, no. 2, pp. 273–278, Mar. 2003.
[7] L. Hyeongcheol and M. Tomizuka, "Adaptive vehicle traction force control for intelligent vehicle highway systems (IVHSs)," *IEEE Trans. Ind.Electron.*, vol. 50, no. 1, pp. 37–47, Feb. 2003.
[8] N. Patel, C. Edwards, and S. K. Spurgeon, "Optimal braking and estimation of tyre friction in automotive vehicles using sliding modes," *Int. J.Syst. Sci.*, vol. 38, no. 11, pp. 901–912, Nov. 2007.
[9] Y. Xinghuo and O. Kaynak, "Sliding-mode control with soft computing: A survey," IEEE Trans. Ind. Electron., vol. 56, no. 9, pp. 3275–3285,Sep. 2009.
[10]Arulmozhiyal.R, and K.Baskaran,"RealTimematlabInterface for Speed Control of Induction Motor Drive using ds PIC 30F4011" International Journal of Computer Applications volume 1 2010.
[11] Ricardo de castro and RuiEsteves,"Wheel Slip Control of EVs Based on Sliding Mode Technique With Conditional Integrators,"IEEE Trans. Ind. Electron., vol. 60, no. 8,Sep. 2013.

 